https://doi.org/10.5194/egusphere-2026-2122
Preprint. Discussion started: 27 April 2026

Understanding uncertainties in Arctic aerosol representation in climate models

Arundathi Chandrasekharan[1], Tommi Bergman[1], Kalle Nordling[1], Meryem Bouchahmoud[1], Joonas Merikanto[1], Risto Makkonen[1]

[1]Finnish Meteorological Institute, 00560 Helsinki, Finland

Correspondence to: Arundathi Chandrasekharan (arundathi.chandrasekharan@fmi.fi)

Abstract. Arctic amplification and its persistent underestimation in climate models underscore the importance of accurate representation of local Arctic feedback processes. Previous studies evaluating model data against measurements showed the importance of including local emissions, such as iodic acid and organic vapours, for an accurate representation of aerosols in the high Arctic. The MOSAiC expedition has produced a full year of data in the high Arctic, providing an opportunity to evaluate the performance of climate models in this region across strongly contrasting seasonal conditions. We evaluate four CMIP6 models and the chemistry-transport model TM5 using this data. CMIP6 models fail to capture the observed seasonal cycle and generally underestimate aerosol number concentration (CN), with the strongest underestimation in summer. To understand the cause of these model deficiencies, we conduct a sensitivity analysis using an ensemble of TM5 experiments by perturbing individual parameters and three reasons were identified. In summer, missing regional new particle formation (NPF) sources are the primary cause of the underestimation. Including methanesulphonic acid driven NPF improved the magnitude and seasonality of simulated CN. In winter and early spring, the model is missing aerosol sources such as blowing snow and lead emissions. During the Arctic haze period, the model underestimates the aerosol background concentration, possibly due to an underestimation of long-range transported aerosols. With cloud condensation nuclei (CCN), we observe a persistent underestimation even during periods of CN overestimation. These results identify gaps in Arctic aerosol representation in climate models that need to be addressed to improve climate projections.

1 Introduction

The Arctic is experiencing unprecedented changes, with warming rates nearly four times the global average (Rantanen et al. 2022). This Arctic amplification is driven by complex feedback mechanisms, is tightly connected to the global Earth system, and influences weather patterns and climate both within and outside the Arctic (Previdi et al. 2021; Malik et al. 2025). Aerosols

https://doi.org/10.5194/egusphere-2026-2122
Preprint. Discussion started: 27 April 2026

play a critical role in Arctic climate change despite their relatively low concentrations compared to mid-latitude regions. Long-range transported aerosols, particularly black carbon and sulphate originating from mid-latitude industrial regions, significantly perturb the Arctic energy balance (Acosta Navarro et al. 2016). On the other hand, regional and local response of natural aerosol and precursor sources modulate feedback processes behind Arctic amplification and contribute to uncertainties in climate projections (Schmale et al. 2021).

Arctic aerosol is a complex seasonal mixture of natural and anthropogenic, as well as primary and secondary aerosols (Schmale et al. 2021). The sources of these aerosols range from long-range transport (Hirdman et al. 2010) to regional or very local small-scale sources, such as leads (Lapere et al. 2024), meltponds (Beck et al. 2021) or blowing snow (Gong et al. 2023). Hence, in addition to the global anthropogenic aerosol sources and large-scale shifts in natural emissions, climate models need to incorporate short-timescale processes, cyclonic activity and local wind-driven sources to improve predictions of Arctic aerosol–cloud interactions (Heutte et al. 2025).

Low pre-existing aerosol surface area, together with cold conditions over the remote Arctic Ocean, creates favourable conditions for new particle formation (NPF). Arctic NPF precursor vapours, including Methanesulphonic acid (MSA), iodic acid and sulphuric acid, exhibit strong seasonal cycles modulated by biogenic activity, solar radiation and sea ice conditions (Boyer et al. 2024). Iodine emitted from sea ice and open-water regions is thought to initiate NPF and has been proposed as a primary driver of late-summer nucleation events over the Arctic Ocean (Baccarini et al. 2020); however, its quantitative contribution remains uncertain due to the lack of halogen chemistry in large-scale models and poorly constrained emission fluxes and process representations (Saiz-Lopez et al. 2025). MSA originating from marine biogenic emissions is a key natural aerosol component in the Arctic and can contribute to the early growth of aerosols (Beck et al. 2021). Hodshire et al. (2019) performed simulations with the GEOS-Chem-TOMAS model with varying assumptions on MSA's effective volatility and potential impact on nucleation. They found a global impact of MSA on total aerosol number concentration to be 112.5% when MSA participates in nucleation, with high enhancement factors at high latitudes. A data-driven approach in Pernov et al. (2024) projected a future seasonal shift in MSA abundance due to changes in atmospheric variables, especially temperature, radiation, boundary layer height and RH. Even over the remote Arctic Ocean, secondary aerosols from high-latitude vegetation can significantly affect cloud condensation nuclei (CCN) concentrations (Tang et al. 2023).

Primary particle sources within the Arctic Ocean include wind-driven sea-spray aerosol (SSA) and blowing snow, as well as small-scale local emissions from leads or melt ponds. Lapere et al. (2023) highlighted substantial uncertainties in Arctic SSA representation within climate models, driven by large variability in source functions and poorly constrained processes and emission size distribution. CMIP6 models failed to reproduce observed seasonal cycles of SSA concentrations, often overestimating mean values by up to an order of magnitude. Recent findings by Gong et al. (2023) showed that blowing snow events occurred over 20% of the time between November and April in the central Arctic, producing substantial concentrations

https://doi.org/10.5194/egusphere-2026-2122
Preprint. Discussion started: 27 April 2026

of fine-mode sea salt aerosols (<300 nm) and increasing CCN levels by up to an order of magnitude above background. Lapere et al. (2024) provided the first estimates of sea spray aerosol emissions from Arctic leads, estimating that these open-water features within sea ice contribute up to 10% of annual sea salt aerosol number emissions and as much as 85% of mass emissions in sea ice regions, highlighting their potentially significant but previously unaccounted role in the Arctic aerosol budget. Fluorescent primary biological aerosol particles (fPBAPs) observed near the North Pole during late summer (Kojoj et al. 2024), likely originated from biologically active ice-free ocean regions, showed strong links to ice-nucleating particles and formation of mixed-phase clouds.

Despite extensive research, major uncertainties remain in Arctic aerosol processes, particularly regarding aerosol-cloud interactions, the contribution of natural sources in a warming climate with declining sea ice, and the impact of shifting atmospheric circulation on transport. Addressing these gaps requires integrated observations, remote sensing, and advanced multi-scale modelling. Advancing understanding of the high-latitude climate system is critical for accurate climate predictions and global policy, as Arctic changes have far-reaching consequences for atmospheric circulation and sea-level rise. In this paper, we address uncertainties in Arctic aerosols using the global chemical transport model TM5. By using a set of simulations with individually perturbed parameters, we quantify the sensitivity of Arctic aerosol to uncertainties in processes and emissions. We utilise the full year of observations from the MOSAiC expedition to constrain the simulation ensemble and identify remaining structural and parametric gaps in the model.

https://doi.org/10.5194/egusphere-2026-2122
Preprint. Discussion started: 27 April 2026

2 Materials and methods

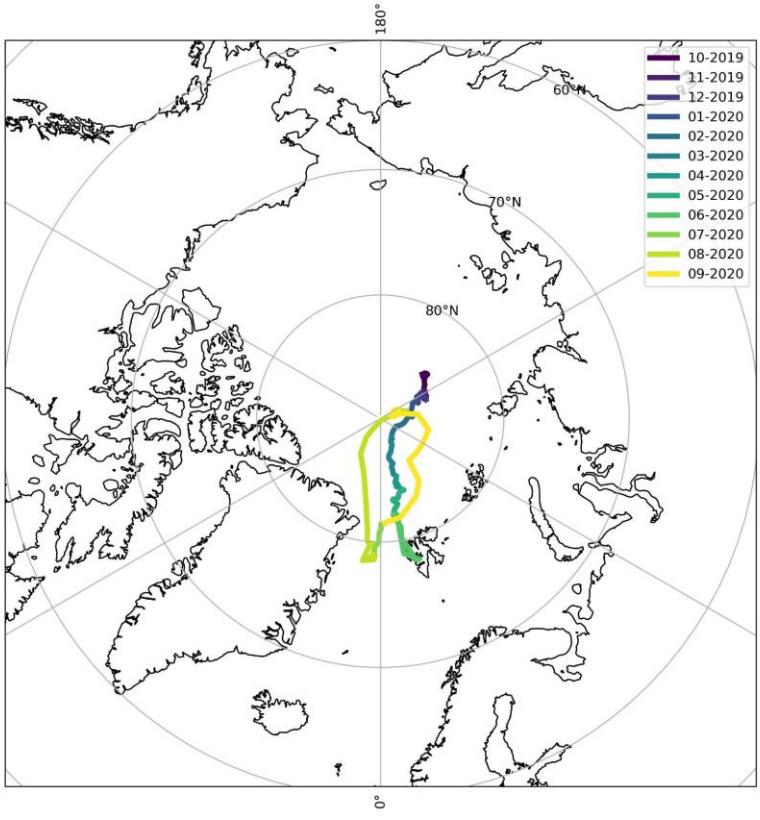

Figure 1: Polarstern path over the months of the MOSAiC campaign

2.1 Chemistry Transport Model TM5-MP

In this study, we used the stand-alone version of the global chemistry transport model (CTM) TM5-MP (Tracer Model 5, Massively Parallel version) (Bergman, Makkonen, Schrödner, Swietlicki, Phillips, Le Sager, and Van Noije 2022; Williams et al. 2017; Van Noije et al. 2014; Huijnen et al. 2010; Krol et al. 2005), referred to hereafter as TM5. The model simulates the evolution of aerosols and trace gases using meteorological and surface fields driven by hourly ERA-5 data (Hersbach et al. 2020) from the European Centre for Medium-Range Weather Forecasting (ECMWF).

https://doi.org/10.5194/egusphere-2026-2122
Preprint. Discussion started: 27 April 2026

2.1.1. Atmospheric chemistry and aerosol processes

A modified version of the CB05 carbon-bond mechanism chemistry scheme, mCB05, is implemented in the model (Williams et al. 2017). The M7 aerosol scheme (Stier et al. 2005; Vignati et al. 2004) implemented in the model is a two-moment scheme with a prescribed geometric standard deviation for each mode, and the number and mass of each mode are calculated at every time step. The name refers to the 7 modes of aerosols, of which 4 are water-soluble, and the other 3 are insoluble. In this work, we use the TM5 version as described in Bergman et al. (2022), with secondary organic aerosols (SOA) added alongside sulphate (SU), organic carbon (OC), black carbon (BC), dust (DU), and sea salt (SS) aerosol components. Ammonium, nitrate, and methanesulphonic acid (MSA) are treated as bulk aerosols, in which the gases immediately condense onto soluble accumulation mode particles on emission. SOA in the model consists of extremely low volatility organic compounds (ELVOCs) and semi-volatile organic compounds (SVOCs). ELVOCs condense on particles depending on the particle surface area of each mode, whereas SVOCs condense on particles depending on the total mass of organic aerosols (OA) existing in each mode. As a result of their treatment in the model, SVOCs mainly contribute to the growth of accumulation mode and coarse mode particles, and ELVOCs contribute to nucleation and early growth of aerosols, as well as the growth of larger aerosol particles (Bergman et al. 2022). The sizes and composition of each of the M7 modes are described in Table 1.

For new particle formation, TM5 combines two nucleation mechanisms: binary sulfuric acid-water nucleation (Vehkamäki et al., 2002) and a boundary-layer nucleation scheme. The boundary-layer nucleation scheme implemented in the model is Riccobono et al. (2014), as described in Bergman et al. (2022). The formation of nucleation mode particles, J in $cm^{-3}s^{-1,}$ is

$$J = K\,[H_2SO_4]^2\,[ELVOC] \quad \text{— — —} \quad \text{(Eq. 1)}$$

where $K = 3.27\times10^{-21}$ cm^6 s^{-1} is the nucleation factor and [H_2S0_4] and [ELVOC] are the gas-phase concentration of sulphuric acid and ELVOCs. Particle formation rate is converted to a 5 nm formation rate using Kerminen and Kulmala (2002) parameterisation.

Dimethyl sulphate (DMS) in the model undergoes oxidation to produce sulphur dioxide and methanesulphonic acid (Huijnen et al. 2010) in the model as follows

DMS + OH ------> 0.75 SO2 + 0.25 MSA — — — (Eq. 2)

Here, OH is the hydroxyl radical, and the reaction rate is 1.0E−39*exp(5820/T), where T is the temperature in kelvins.

Cloud Condensation Nuclei (CCN) calculation in TM5 is based on equation 10 from Petters and Kreidenweis (2007). CCN is a climate-relevant variable; it is a fraction of ambient aerosols that can participate in cloud droplet formation. The ability

https://doi.org/10.5194/egusphere-2026-2122
Preprint. Discussion started: 27 April 2026

of an aerosol particle to act as a CCN depends on its size and chemical composition, as well as on the ambient supersaturation. A fraction of accumulation and coarse mode particles can act as CCN.

2.1.2 Aerosol emissions and precursors

The evolution of the aerosol population in TM5 depends on the modelled and prescribed emissions. The anthropogenic emissions and the natural aerosol baseline for the model are from the CMIP6 emission dataset (T. van Noije et al. 2021; T. P. C. van Noije et al. 2014; Lamarque et al. 2013; van Vuuren et al. 2011), following the Shared Socioeconomic Pathway 3-7.0 scenario (Gidden et al. 2019) for the studied period (2019-2020). DMS emissions over land are calculated as described in Spiro et al. (1992), and oceanic DMS emissions are calculated based on Lana et al. (2011), masked by prescribed 1-degree sea ice cover. Wind-driven sea spray emissions from breaking waves (SSA) in TM5 are based on Gong (2003), with a temperature dependent size distribution as described in Van Noije et al. (2021). Biogenic emissions of non-methane volatile organic compounds (NMVOCs) are based on Guenther et al. (2012). The chemistry setup and other emissions in the model are described in detail in Huijnen et al. (2010) and Van Noije et al. (2014).

M7 modes in TM5-MP	Geometric deviation (σ)	Mixed	Insoluble
Nucleation (0-0.005 µm)	1.59	SU, SOA	
Aitken (0.005-0.05 µm)	1.59	SU, OC, BC, SOA	OC, BC, SOA
Accumulation (0.05-0.5 µm)	1.59	SU, OC, BC, SOA, SS, DU	DU
Coarse (>0.5 µm)	2.0	SU, OC, BC, SOA, SS, DU	DU

https://doi.org/10.5194/egusphere-2026-2122
Preprint. Discussion started: 27 April 2026

Table 1: M7 aerosol scheme used in TM5-MP, the dry radius of the particles and the standard deviation (σ) are noted in the corresponding mode. The components in each mode are modelled as a tracer containing the total mass of the component, and each mode has an additional tracer with the total number of particles.

2.2 Simulations

We ran 11 simulations for this study. For all simulations, the model was run from October 2019 to September 2020 with a 9-month spin-up period, at a horizontal resolution of 3° longitude by 2° latitude and vertical resolution of 34 hybrid sigma-pressure levels. The model output was analysed at a 1-hour temporal resolution. For direct comparison between the model and the MOSAiC observational data, nearest-neighbour interpolation based on the vessel's hourly average position was used. As the measured aerosol diameter had a lower cutoff of 3 nm, the same was implemented for the model output.
A brief description of the simulations is given in Table 2, and they are discussed in detail in the following subsections.

2.2.1 Control simulation

The control simulation, named BASECASE, is used as the reference to understand the sensitivity of TM5 to different aerosol parameters. The control simulation is based on TM5 as described in Sect. 2.1, but has an alternative treatment of MSA. To account for MSA contribution to early aerosol growth, we extend the description of MSA with the volatility mechanism described in Bergman et al. (2022). Instead of treating MSA as only bulk aerosol mass, we assume MSA to behave as ELVOC-like or SVOC-like, with a pre-defined fraction of MSA as ELVOC/SVOC. Similar to Bergman et al. (2022), the ELVOC-like (SVOC-like) MSA fraction partitions to the aerosol phase according to pre-existing aerosol surface area (organic mass). In addition, we assume that ELVOC-like MSA can participate in nucleation and early growth (section 2.1).

2.2.2. Nucleation scheme

We perturb the nucleation rate to see the effect of nucleation events on the aerosol profile. NUCLRATE_HIGH and NUCLRATE_LOW use the same setup as the BASECASE simulation, but with the nucleation rate described in Eq. (1) multiplied by 10.0 and 0.1, respectively.

Earlier iterations of the model used nucleation schemes driven only by the concentration of gaseous sulphuric acid (Van Noije et al. 2014).To assess the sensitivity of simulated aerosol concentrations to new particle formation, we also tested a different boundary-layer nucleation mechanism. Experiment SO4NUCL uses a nucleation scheme based on Sihto et al. (2006) with sulphuric acid as the only aerosol precursor gas contributing to nucleation. The formation rate of nucleation mode particles J in $cm^{-3}s^{-1}$ is given by

$J = A\ [H_2SO_4]$ — — — — (Eq. 3)

https://doi.org/10.5194/egusphere-2026-2122
Preprint. Discussion started: 27 April 2026

where A = 1.7 x10^{-6} and [H_2SO_4] is the gas phase concentration of sulphuric acid.

2.2.3 MSA volatility

We carried out a sensitivity test to see how the MSA volatility description affected the modelled aerosol concentrations. For the BULKMSA experiment, we run the model with MSA being treated as a bulk tracer that immediately condenses on the soluble accumulation mode, as described in Section 2.1. The MSA_ELVOC and MSA_SVOC are used to understand how important the contribution of organic compounds is to nucleation and early growth. MSA_ELVOC treats all available MSA as ELVOC-like gases. In the MSA_SVOC experiments, all the MSA is treated as SVOC-like gases.

2.2.4 Natural aerosols and aerosol precursors in the Arctic

Near the poles, dimethyl sulphate (DMS) is one of the main sources of naturally occurring secondary aerosol due to the pristine environment of the region. In TM5, it undergoes oxidation to produce sulphate and MSA (see Eq. 2), both of which contribute to aerosol nucleation and growth processes. DMSHIGH and DMSLOW experiments are used to see how changes in the concentration of aerosol precursor gases affect the aerosol concentrations. The DMS emissions, based on Lana et al. 2011, are multiplied by 10.0 and 0.1, respectively, for DMSHIGH and DMSLOW cases.

Sea spray emissions are a source of primary aerosols. In TM5, they are emitted to coarse and accumulation mode(see Table 1) and so, affect both the number concentration and coagulation sink, as these are larger particles that can be condensed on. In the SS_HIGH and SS_LOW experiments, we multiply the emissions by a factor of 10.0 and 0.1, respectively.

Experiment	Description
BASECASE	Nucleation scheme used is Riccobono et al. (2014) as described in Bergman et al. (2022) (Eq. 1) 50% MSA emitted is treated as ELVOC-like, and 50% is treated as SVOC-like.
SO4NUCL	Nucleation scheme used is based on Paasonen et al. (2010), with nucleation only driven by sulphuric acid concentration (Eq. 2)
BULKMSA	Nucleation scheme is the same as BASECASE, but MSA is treated as a bulk tracer and does not participate in chemistry
DMS_HIGH	BASECASE with the DMS emission in the model multiplied by a factor of 10

https://doi.org/10.5194/egusphere-2026-2122
Preprint. Discussion started: 27 April 2026

DMS_LOW	BASECASE with the DMS emission in the model multiplied by a factor of 0.1
MSA_ELVOClike	Nucleation scheme is the same as in BASECASE. 100% of MSA is treated as ELVOC-like
MSA_SVOClike	Nucleation scheme is the same as in BASECASE. 100% of MSA is treated as SVOC-like
NUCLRATE_HIGH	BASECASE with the nucleation rate multiplied by 10
NUCLRATE_LOW	BASECASE with the nucleation rate multiplied by 0.1
SS_HIGH	BASECASE with the SSA emission multiplied by 10
SS_LOW	BASECASE with the SSA emission multiplied by 0.1

Table 2. Description of the experiment setups

2.3 Datasets

2.3.1 CMIP6 datasets

We compare our model output with CMIP6 data from four Earth System Models (ESMs), namely, CESM2, MRI-ESM2, MIROC-ES2H and UKESM1. The data was accessed from the Earth System Grid Federation (ESGF; (Cinquini et al. 2014). We chose the models based on the availability of *conccn,* which is the aerosol number concentration (CN). All of the models have data from the experiment *historical,* where coupled climate models are forced with historical drivers for greenhouse gases, land use and aerosols(Eyring et al. 2016). CESM2 and MRI-ESM2 also have *conccn* available for the *AMIP* experiment, which have prescribed sea surface temperature (SST) and sea ice cover (SIC) based on observations. The *historical* experiments run from 1850 to 2014 and do not include the years of the MOSAiC experiments. So, we use data from 2005 to 2014 for our analysis, as this gives a range of values to understand the behaviour of the model over different conditions. Since the spread of the model values is used, not just a mean value, this makes a fairer comparison. Comparison between the *historical* and *AMIP* data for these models will help understand the atmospheric component of the model separately, and can be used to make sense of discrepancies between modelled and measured values.

https://doi.org/10.5194/egusphere-2026-2122
Preprint. Discussion started: 27 April 2026

The treatment of aerosols in the CMIP6 models used is as listed

- CESM2 uses the MAM4 (Modal Aerosol Module 4) aerosol scheme. Aerosol components include sulphate, sea salt, land dust and primary and secondary organic matter. Liu et al. (2016) and Danabasoglu et al. (2020) describe the model setup and its aerosol scheme in detail.

- MIROC uses the Spectral Radiation-Transport Model for Aerosol Species (SPRINTARS) aerosol scheme. Sulphate and precursors (SO2 and DMS), BC, OC, sea salt, soil dust, prognostic precursor gases of organic matter and diagnostic oceanic primary and secondary organic matter (Hajima et al. 2020; Takemura et al. 2005)

- MRI-ESM2 uses the aerosol transport model MASINGAR (Model of Aerosol Species IN the Global AtmospheRe). Sulphate, carbonaceous, mineral dust and sea salt are the aerosol components modelled. Sea salt aerosol emission is only wind dependent in the model, unlike the other models, where it also depends on the sea surface temperature(Adachi et al. 2013; Tanaka et al. 2003; Yukimoto et al. 2019)

- UKESM1 uses the GLOMAP aerosol scheme, in which the aerosol components are sea salt, sulphate, BC and OC. The model also contains mineral dust, which is externally mixed with the GLOMAP aerosols. The scheme is explained in detail in Mulcahy et al. (2023, 2020).

2.3.2 MOSAiC expedition

For this study, we focus on the observational data from the Multidisciplinary drifting Observatory for the Study of Arctic Climate (MOSAiC) expedition that took place from 20th September 2019 to 12th October 2020 on the German research icebreaker Polarstern. The vessel was frozen into sea ice and passively drifted with the Arctic sea ice for most of the duration of the expedition. The design of the experiment and the atmospheric conditions during the expedition are detailed in (Shupe et al. 2022).

Here, we use three datasets for comparison with our model output. The aerosol number concentration (CN) was measured using a Condensation Particle Counter, which measures the concentration of particles between 3 nm and 1 μm. The values were measured every 10s, and the corrected data were available at 1-minute frequency with the polluted points flagged. The concentration of CCN at 0.20% supersaturation was measured using a Cloud Condensation Nuclei Counter(CCNC); this data is available only till May 2020 due to instrument failures. The instruments used and the processes involved in creating these datasets are discussed in detail in (Heutte et al. 2023; Boyer et al. 2023). We also looked at aerosol precursor gases such as Sulphuric Acid (H2SO4), Iodic Acid (HIO3) and Methanesulphonic Acid (MSA) values measured using a Nitrate Chemical

https://doi.org/10.5194/egusphere-2026-2122
Preprint. Discussion started: 27 April 2026

Ionisation Mass Spectrometer (NO3-CIMS) (Boyer et al. 2024). For the datasets used, all the points marked as polluted were ignored for analysis and plotting.

3. Results

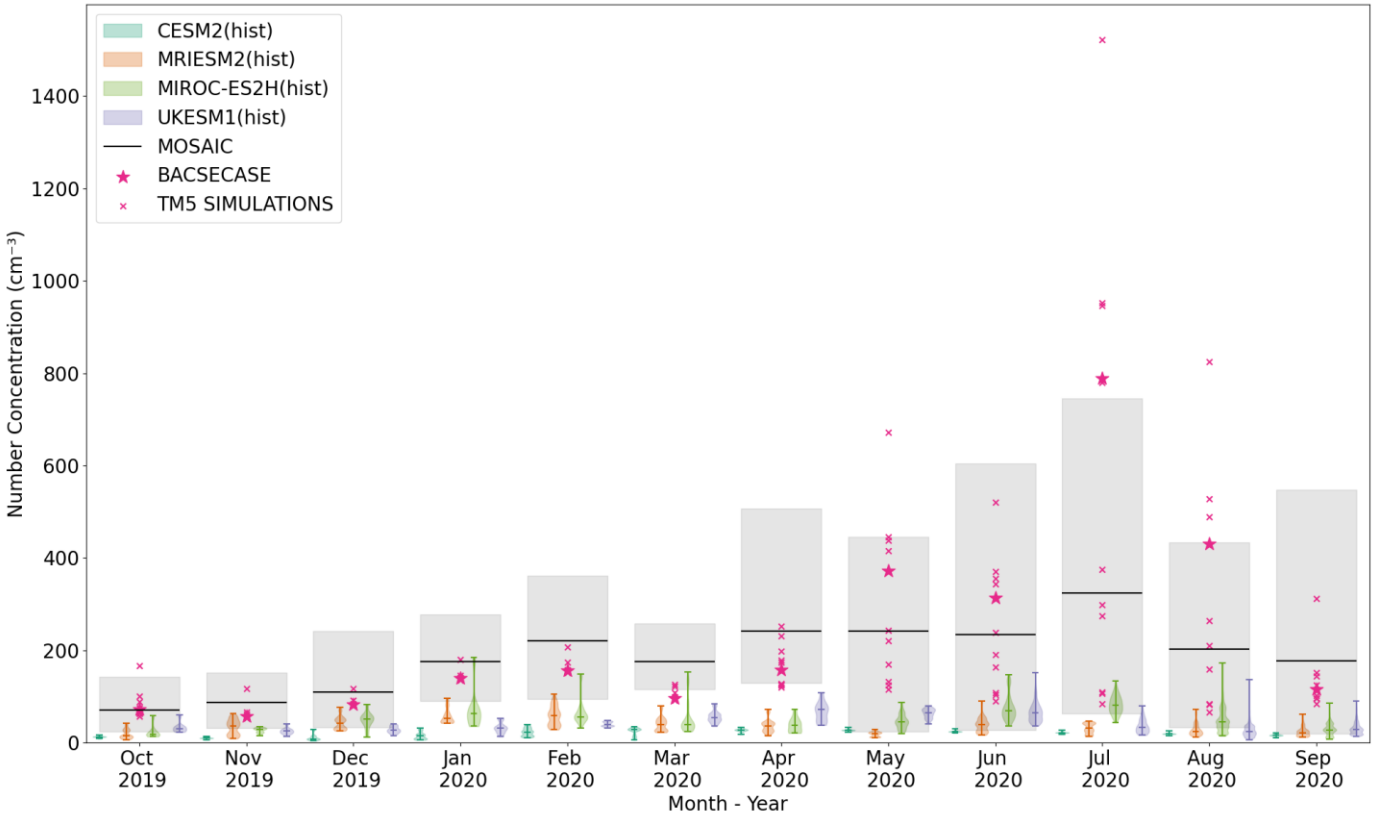

Fig 2: Comparison of monthly average CN between CMIP6 models along the MOSAiC track, TM5 values and measured values during the expedition. The violins show CN for the CMIP6 models are from monthly averages from 2005 to 2014. The black line represents the monthly average values from the MOSAiC expedition data, with the grey shaded region showing the 10th to 90th percentile values. The pink star represents the monthly average CN from the TM5 model output. The pink crosses mark the monthly values of all the experiments other than BASECASE

3.1 Representation of aerosols in the Arctic in CMIP6 models

In Fig. 2, we see that the CMIP6 models considered, CESM2, MRIESM2, MIROC-ES2H and UKESM1, simulate lower CN values than the TM5 model output and the MOSAiC measurements. The variability in the monthly averages differs between

https://doi.org/10.5194/egusphere-2026-2122
Preprint. Discussion started: 27 April 2026

the four models. All four analysed CMIP6 models underestimate observed monthly averaged CN concentrations, while TM5 both underestimates or overestimates the observed monthly CN, depending on the experiment. CESM2 has the lowest value for all months except May 2020, with the values staying very close to zero throughout the year. CN in MIROC-ES2H and UKESM1 show more variability. We see a spread in the simulated values for MIROC-ES2H throughout the year, whereas with UKESM1, the spread in values is only observed in summer. Comparing CMIP6 models with TM5 model output and MOSAiC observations, there is a significant gap between these values. In the winter months, the gap between CMIP6 models, TM5 and MOSAiC is lower than in the summer.

The CMIP6 models do not capture the observed seasonal cycle of CN of the MOSAiC expedition. During summer, we can see that the mean observed CN is outside the range of the CMIP6 mean values. This could be due to missing processes or incorrect representation of sea ice cover and/or sea surface temperature in the models. From Fig. S1, where CN from both *historical* and *AMIP* experiments are plotted for CESM2 and MRI-ESM2, we can see that the latter has better agreement with observations for CESM2. The main difference between the experiments is that the *AMIP* runs use observed SIC and SST for the plots, while the *historical* experiments are not constrained, and this could be the main reason for the values being closer to the observations. While the winter values remain the same between the hist and *AMIP* runs, we find that from late spring to early autumn (April 2020 – September 2020), the *AMIP* simulations are closer to the observations and have a larger spread in values. These variables are important parameters when calculating SS and DMS emissions. For MRI-ESM2, both historical and *AMIP* experiments have similar values. Since SS emissions in the model do not depend on SST (Tanaka et al. 2003; Adachi et al. 2013), this could point to the modelled SIC being close to observations. Lapere et al. found that SS in CMIP6 models are not sensitive to SST, so most of the differences are likely caused by changes in SIC between the simulations. While this difference does partly explain the much lower CN values in CMIP6 models, the gap between the CMIP6 models and observations is still significant and probably caused by missing processes, such as incorrect emission of DMS or contribution of MSA to aerosol formation, that we discuss in the following sections.

https://doi.org/10.5194/egusphere-2026-2122
Preprint. Discussion started: 27 April 2026

Fig. 3: Violin plot of the daily average CN from the MOSAiC expedition and the simulation, BASECASE, along the MOSAiC track. MOSAiC and BASECASE values are plotted as the left and right half violin, respectively, with the shaded area showing the probability density function of the CN values. The horizontal lines at the top and bottom of the violins represent the maximum and minimum, and the line in the middle is the median. The four subplots show the sensitivity of the model to perturbing parameters related to MSA volatility (a), DMS emissions (b), Nucleation (c) and Sea Spray emissions (d), with the lines showing the median values of the experiment and the shaded region showing the difference between the lowest and highest values.

3.2 Aerosol seasonal cycle

3.2.1 Aerosol number concentration

In Fig. 3, the observed CN values show a seasonal cycle due to differences in aerosol sources; we see that this is mostly captured in the BASECASE simulation, with the modelled minimum occurring a month later. MOSAiC measurements and BASECASE simulation reach their maximum in July. The minimum is a month apart, in October for MOSAiC and in November for BASECASE. This simulation underestimates CN concentrations in winter and early spring (November 2019 - April 2020) and overestimates from late spring till the end of autumn (October 2019, May 2020 - September 2020). During

https://doi.org/10.5194/egusphere-2026-2122
Preprint. Discussion started: 27 April 2026

winter, most of the aerosols in the Arctic are transported from lower latitudes (Boyer et al. 2023). Since the model does not appear to be sensitive to changes in natural aerosols, our model runs likely reflect these findings. Local processes are the dominant source of aerosols in the Arctic during summer (Moschos et al. 2022; Schmale et al. 2021). As the parameters chosen for this study mostly affect local processes, we see a bigger spread in the simulated CN concentration in summer.

From January 2020 to April 2020, MOSAiC daily CN is typically higher than in any TM5 experiment (see Fig 3). Unlike MOSAiC, TM5 often has daily CN very close to zero during these months. This period corresponds to the occurrence of Arctic Haze, which results in a higher background aerosol concentration (Boyer et al. 2023). We speculate that this discrepancy may arise because TM5 does not capture this characteristic phenomenon. In contrast, during the summer months, TM5 predicts a higher daily minimum, whereas observations show days when CN concentrations approach zero. The main cause of increased CN values in the summer is the inclusion of MSA in NPF. However, as NPF events occur over a period of hours and do not occur every day, we can assume that this is not the cause of the increased background aerosol concentration. In Lapere et al. (2023), among Alert, Villum and Zeppelin stations, which are close to Polarstern's path during this period, positive biases in sea spray emissions were observed in Alert and Villum for CMIP6 models. From this, we can assume that the SSA schemes in models result in a higher aerosol baseline than observations.

When looking at the CN values, all experiments except SS_HIGH(Fig. 3d), SO4NUCL(Fig. 3c), BULKMSA(Fig. 3a) and MSA_SVOClike (Fig. 3a) follow the same seasonal cycle as BASECASE and reach the maximum and minimum in the same months. The CN for SS_HIGH is closer to MOSAiC in the winter months, but does not reflect the observed seasonal cycle in the summer. We can speculate that the lower CN concentration for SS_HIGH in summer is due to the increase in concentration of the large SSA particles, resulting in a bigger condensation and coagulation sink. In Fig. S3, where the fraction of nucleation mode particles which move into Aitken mode is plotted, we can see that the SS_HIGH case has a much smaller fraction due to the nucleation mode particles coagulating on the larger particles, such as SSA. This, in turn, reduces the number of nucleation mode particles that can grow into Aitken mode particles. When looking at the role of sea spray emissions, we see that SS_HIGH and SS_LOW experiments do not always show opposite changes; rather, there is a non-linear response of CN to changes in emissions. The modelled CN values for both cases are higher than BASECASE in April and August. We will look at this in detail in the next section.

In winter, CN for BULKMSA (Fig. 3b), SO4NUCL (Fig. 3c) and MSA_SVOClike (Fig. 3c) are similar to BASECASE and follow the same trend. However, in summer, the CN for these experiments are lower than both the BASECASE and MOSAiC. In this study, only these three experiments have no contribution from MSA to nucleation. Nucleation in SO4NUCL is only driven by the concentration of gaseous sulphuric acid. BULKMSA treats MSA as a bulk aerosol mass tracer and MSA_SVOClike where all MSA is assumed to be SVOC-like and only participating in particle growth.

https://doi.org/10.5194/egusphere-2026-2122
Preprint. Discussion started: 27 April 2026

During the MOSAiC expedition, measured ambient sulphuric acid concentration in the summer months was less than 1* 10^6 /cm^3, the threshold above which nucleation occurs in the atmosphere in the absence of other relevant aerosol precursors (Sipilä et al. 2010; Boyer et al. 2024). Measured sulphuric acid concentration peaked during the Arctic haze, which occurred between November 2019 and May 2020 during the expedition. In the Arctic, DMS oxidation has been shown to favour production of MSA over sulphate (Shen et al. 2022), but in the model, DMS oxidation favours sulphate formation (Eq 3). This shows that using only sulphuric acid driven NPF schemes in the Arctic could be limiting the performance of the model. As MSA and Iodic acid are the primary drivers of nucleation in the summer in the high Arctic (Boyer et al. 2023), we can speculate that improved representation of SOA formation from marine sources is crucial for accurately modelling the aerosol population in the Arctic. For our BASECASE, we assumed that 50% of MSA acts ELVOC-like, contributing to new particle formation and early growth. Fig. 3 shows that this leads to an overestimation of CN, even though the modelled MSA concentration is lower than the measurements by about one order of magnitude. In Fig. 3a, we also see that the jump and overestimation in CN concentration are bigger when switching from all MSA acting as SVOC-like to 50% of MSA acting as SVOC-like than when 50% of MSA acting as ELVOC-like is switched to 100% of MSA acting as ELVOC-like. The treatment of MSA as ELVOC-like and contributing to nucleation and early growth shows better agreement with observations for capturing the seasonal cycle. From this, we can see that including the role of MSA in NPR and growth is important for capturing the aerosol seasonal cycle in the Arctic.

We find no experiment that is consistently close to the MOSAiC observations. In winter, SS_HIGH (Fig. 3d) is closest to MOSAiC, but this simulation performs poorly in the summer. This could point to the model lacking a source of aerosols in winter that would have the same drivers as SSA (SIC, SST and wind speed). Blowing snow (Gong et al. 2023) or SSA emission from leads (Lapere et al. 2024; Emme and Horowitz 2025) are possible sources which could make the model perform better in winter. In summer, DMS_LOW and NUCLRATE_LOW almost overlap for all the months except May and June 2020, and have values close to and follow a similar pattern as the MOSAiC observations in summer (see Fig. S2). Both experiments make similar changes to the nucleation rate. NUCLRATE_LOW reduces the nucleation rate to 1/10th of BASECASE. With DMS_LOW, the DMS emissions are reduced to 1/10th of BASECASE. Reduction of DMS in the Arctic means that this in turn reduces the MSA and subsequently ELVOC concentration, leading to nucleation rate becoming roughly 1/10th compared to the BASECASE. This points to the potential role of MSA in nucleation and early growth of aerosols in the Arctic, but to a lesser extent than our initial best assumption, BASECASE. However, the overestimation of CN values in July, even for these cases, and the difference between observed and modelled fraction of MSA mean that its role has to be studied further before we come to a conclusion.

https://doi.org/10.5194/egusphere-2026-2122
Preprint. Discussion started: 27 April 2026

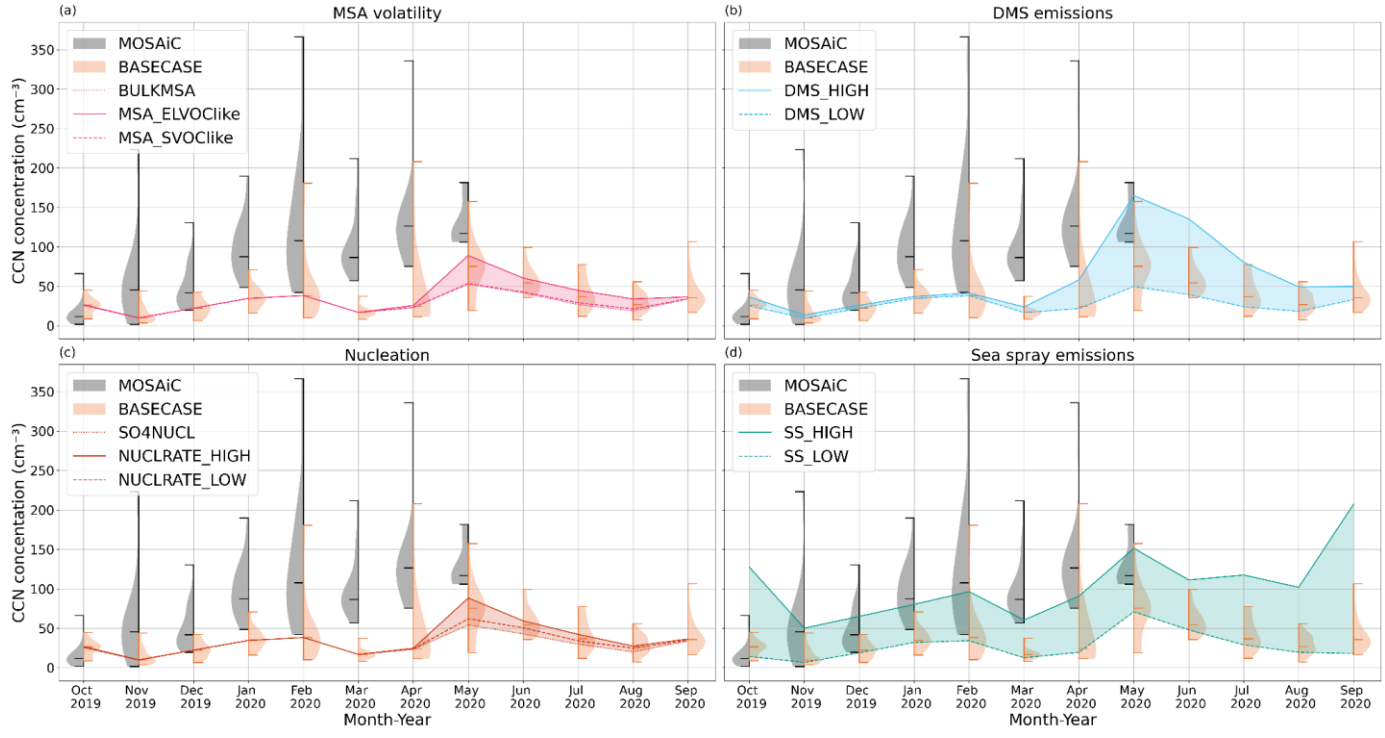

Fig. 4: Violin plot of the daily average CCN at 0.2% supersaturation from the MOSAiC expedition and the simulation, BASECASE, along the MOSAiC track. MOSAiC and BASECASE values are plotted as the left and right half violin, respectively, with the shaded area showing the probability density function of the CCN at 0.2% supersaturation values. The horizontal lines at the top and bottom of the violins represent the maximum and minimum, and the line in the middle is the median. There are four subplots showing the sensitivity of the model to perturbing parameters related to MSA volatility (a), DMS emissions (b), Nucleation (c) and Sea Spray emissions (d), with the lines showing the median values of the experiment and the shaded region showing the difference between the lowest and highest values. The observed CCN data are available only until May 2020 due to instrument failure (Heutte et al. 2023).

3.2.2 CCN concentration

Figure 4 shows that the CCN values for BASECASE are lower than the MOSAiC measurements for all months except October 2019. The CCN for BASECASE in March 2020 is lower than the measurements, with the maximum modelled value well below the minimum measured values. Apart from SS_HIGH (Fig. 4d), all the other simulations are underestimating CCN values in winter, as with the CN values (Fig 3). The highest CCN concentration is for SS_HIGH in all months except May 2020 and June 2020, when DMS_HIGH has the highest value. The lowest CCN concentrations are for DMS_LOW

https://doi.org/10.5194/egusphere-2026-2122
Preprint. Discussion started: 27 April 2026

(Fig. 4b) from May 2020 to August 2020 and SS_LOW (Fig. 4d) for the other months. CCN values are very sensitive to changes in SS emissions. SSA are emitted as larger particles, in the accumulation and coarse mode in the model, which, with their high solubility, directly contribute to CCN formation. As with the CN, modelled CCN is mostly sensitive to changes in parameters from late spring to summer (May 2020 – August 2020).

Other than SS emissions, the model is most sensitive to changes in DMS concentrations. We see a slightly higher CCN value in summer, but from early spring, we see the CCN values for DMS_HIGH (Fig. 4b) increasing. This period corresponds to increasing DMS emissions, with the model predicting higher gaseous sulphuric acid concentrations as well. This can be the result of increased MSA and sulphuric acid concentration, helping with particle formation as well as growth to create particles that can act as CCN.

From May 2020 to August 2020, while CCN for SS_HIGH is much higher than for BASECASE, there is no proportionate decrease for SS_LOW (see Fig. 4d), which stays close to BASECASE. The data points to the limiting factor for CCN formation for these months to be DMS concentration. New particle formation and MSA volatility also show similar non–linear changes. While NUCLRATE_HIGH (Fig. 4c) and MSA_ELVOClike (Fig. 4a) have similar values, NUCLRATE_LOW (Fig. 4c) has higher values than MSA_SVOClike (Fig. 4(a)). This shows that a higher proportion of MSA acting ELVOC-like is more conducive to CCN formation than a higher concentration of smaller particles formed as a result of NPF events.

There is a discrepancy between the CN and CCN predicted by the model. When compared to MOSAiC measurements, the CCN values are lower even during periods where the corresponding CN values are higher than the measurements. This could point to biases in prescribed emission size distributions or primary emission strength, insufficient simulated growth of sub-

https://doi.org/10.5194/egusphere-2026-2122
Preprint. Discussion started: 27 April 2026

350 CCN-sized particles to CCN sizes, or biases in aerosol hygroscopicity.

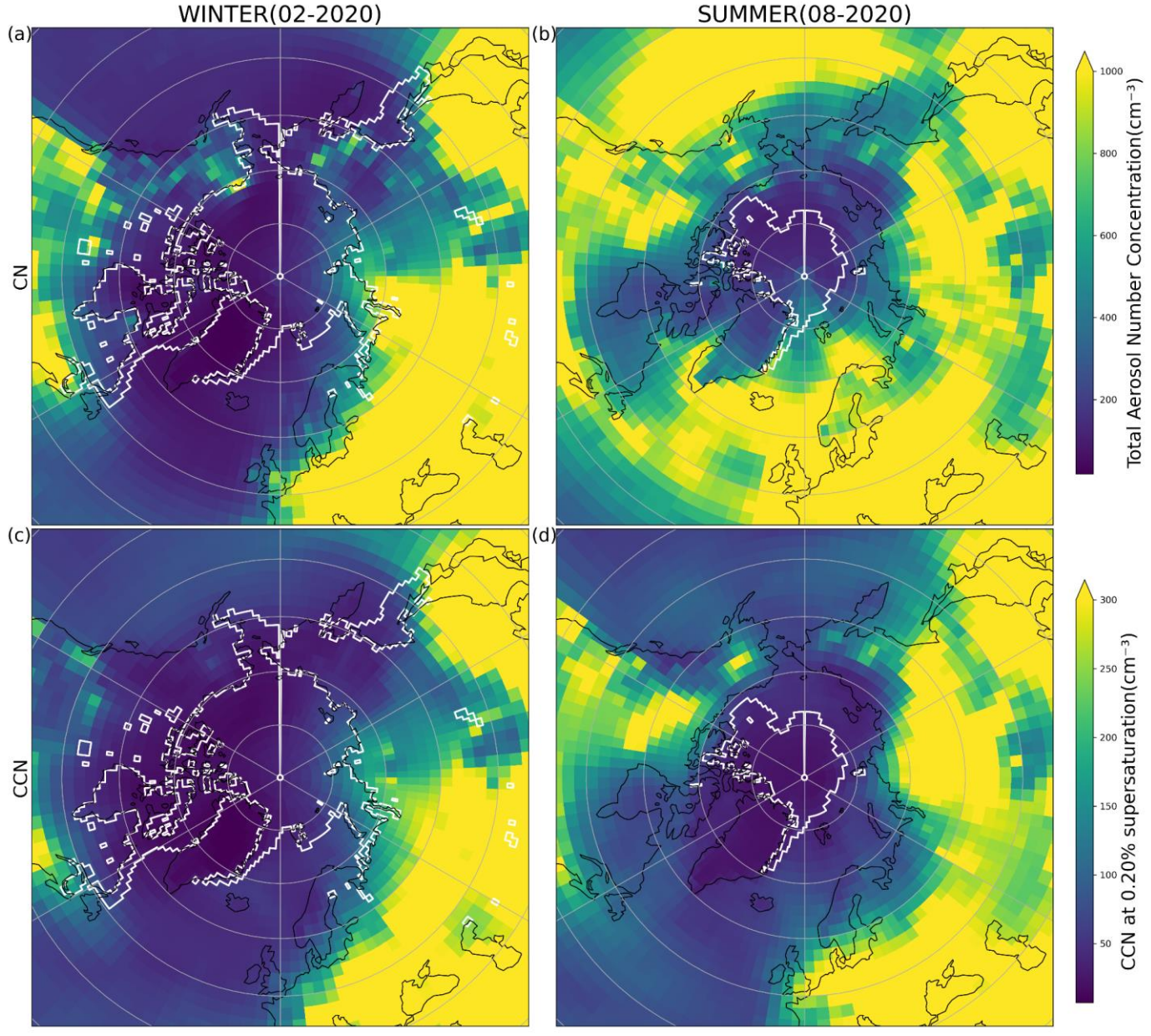

Fig. 5: Spatial distribution of monthly average CN for February 2020 (a) and August 2020 (b), and CCN for February 2020 (c) and August 2020 (d) from the BASECASE experiment. The white line shows the regions with at least 25% sea ice cover on average for the month.

https://doi.org/10.5194/egusphere-2026-2122
Preprint. Discussion started: 27 April 2026

3.3 Spatial variation of aerosol sensitivity

Figure 5 shows the spatial distribution of CN and CCN for a summer and winter month, giving an overview of how the values are affected by the variation in conditions over the Arctic. When comparing the CN and CCN for the two months, we can see that the regions free of sea ice cover have higher CN values since both the DMS and SS parameterisations calculate emissions based on the fraction of open ocean in a grid.

In February 2020, most of the Arctic was covered by sea ice, which resulted in low CN values and a lower sensitivity of the model to altering the chosen parameters. CN values are below 200 cm^{-3} in the Arctic, except for some parts of the continental Arctic (Fig. 5a). In February, the CN (Fig. 5a) and CCN (Fig. 5c) values have a similar spatial pattern; regions with higher CN also have higher CCN concentration.

In August 2020 (Fig. 5b), a summer month, we see regions of much higher CN concentrations, with Svalbard, Iceland and the southern part of Greenland having values higher than 100 cm^{-3}. Unlike in February, the CN and CCN values do not have a similar spatial distribution. Over land, high CN corresponds to high CCN, but this is not the case over the open ocean. As discussed in the earlier section, higher SSA leads to higher CCN in TM5. The other major source of aerosols over the Arctic Ocean is the products of DMS oxidation. In the previous section, we saw that even though NPF improved the CN, the CCN did not see a corresponding increase.

From Figs. 6 and 7, we see that CCN values change as expected with changes in the parameters. However, the changes in CN values are complex, with some parameters resulting in a change in the same direction when increased or decreased (Fig. 6 (e and f) and 7 (q and r)). This could be because CCN concentration is mainly dependent on emission and deposition rates, whereas condensation and coagulation sinks are also involved in determining CN concentration.

The CN in February is around 200 cm^{-3} and shows low sensitivity to changes in parameters (Fig. 6), staying within ± 25% for most experiments. Only the increase in SSA emissions seems to have an impact on CN values in the Arctic. For August, as seen in Fig. 3, the values are more sensitive to changes in the selected parameters. The DMS_HIGH (Fig. 6f) experiment has a smaller increase in values near the Polarstern path, and the increase seems close to the NUCLRATE_HIGH (Fig. 6j) experiment in parts of the Arctic. We also see a region which has low sensitivity from the Beaufort Sea to the East Siberian Sea.

In SO4NUCL, the CN concentration in the Arctic is lower in both February 2020(Fig.6a) and August 2020 (Fig.7a). However, it shows an increase over patches in North Asia and North America, which are areas with higher importance for sulphuric acid than ELVOC for nucleation. When looking at BULKMSA (Fig. 6a, 7a), we see consistently lower values over

https://doi.org/10.5194/egusphere-2026-2122
Preprint. Discussion started: 27 April 2026

the Arctic. As discussed in Section 3.2, this shows the importance of aerosol precursors other than SA, such as MSA, in the Arctic.

In Fig.7, SS_HIGH (Fig. 7q) and SS_LOW (Fig. 7r) have higher CN values in summer from the Beaufort Sea to the East Siberian Sea, which is the same region which has low sensitivity in February. This area is near the open ocean and is in an area not covered by the Polarstern path. Even though CN increases over the same areas for both simulations, the causes are different. When we reduce SS emissions, the reduction in the number of bigger particles reduces the condensation sink. This results in a higher number of smaller particles. For SS_HIGH, even though the increase in SS particles increases the condensation sink, since the region does not have SIC, the increase in the number of particles due to increased SS emissions makes up for it.

When we look at the spatial variation of CCN0.2, the changes are lower, with most of the central Arctic showing no sensitivity to changes in parameters. In February 2020, the model was only sensitive to an increase in DMS (Fig. 7h) or a change in SS (Fig. 7s, 7t). The variation for all the other cases is close to zero. In summer, we see a similar pattern, but amplified. But here again, we notice that the changes from the BASECASE are very small for all cases except for changes in DMS (Fig. 8g,8h) and SSA (Fig. 8s,8t).

https://doi.org/10.5194/egusphere-2026-2122
Preprint. Discussion started: 27 April 2026

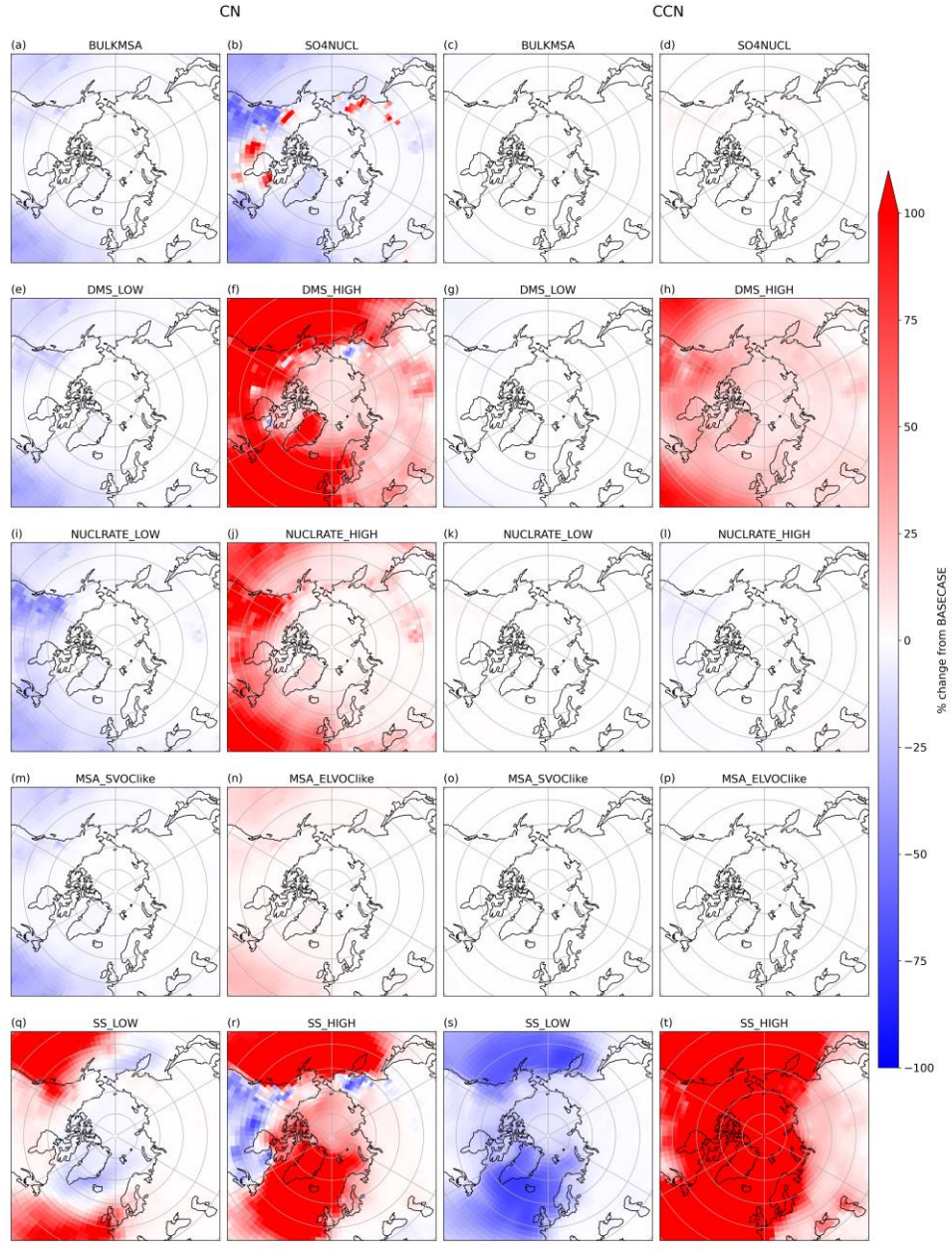

Fig 6: Spatial plot of percentage change from BASECASE of CN and CCN in February 2020 for the simulations. The first two columns are CN values, and the next two columns are CCN values. The change is calculated using the monthly average values.

https://doi.org/10.5194/egusphere-2026-2122
Preprint. Discussion started: 27 April 2026

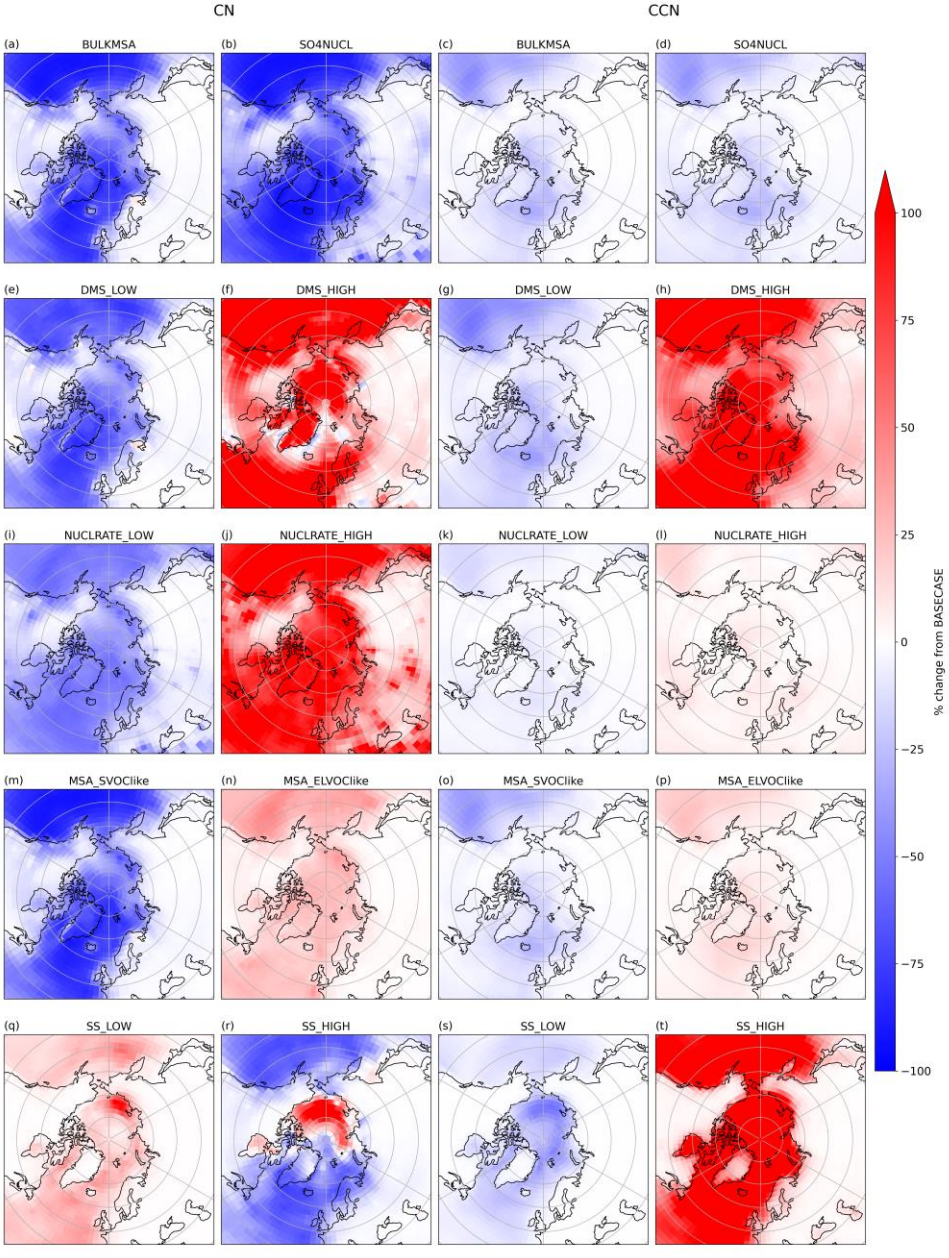

Fig 7: Spatial plot of percentage change from BASECASE of CN and CCN in August 2020 for the simulations. The first two columns are CN values, and the next two columns are CCN values. The change is calculated using the monthly average values

https://doi.org/10.5194/egusphere-2026-2122
Preprint. Discussion started: 27 April 2026

405 **3.4 Detection of extreme aerosol events in the Arctic**

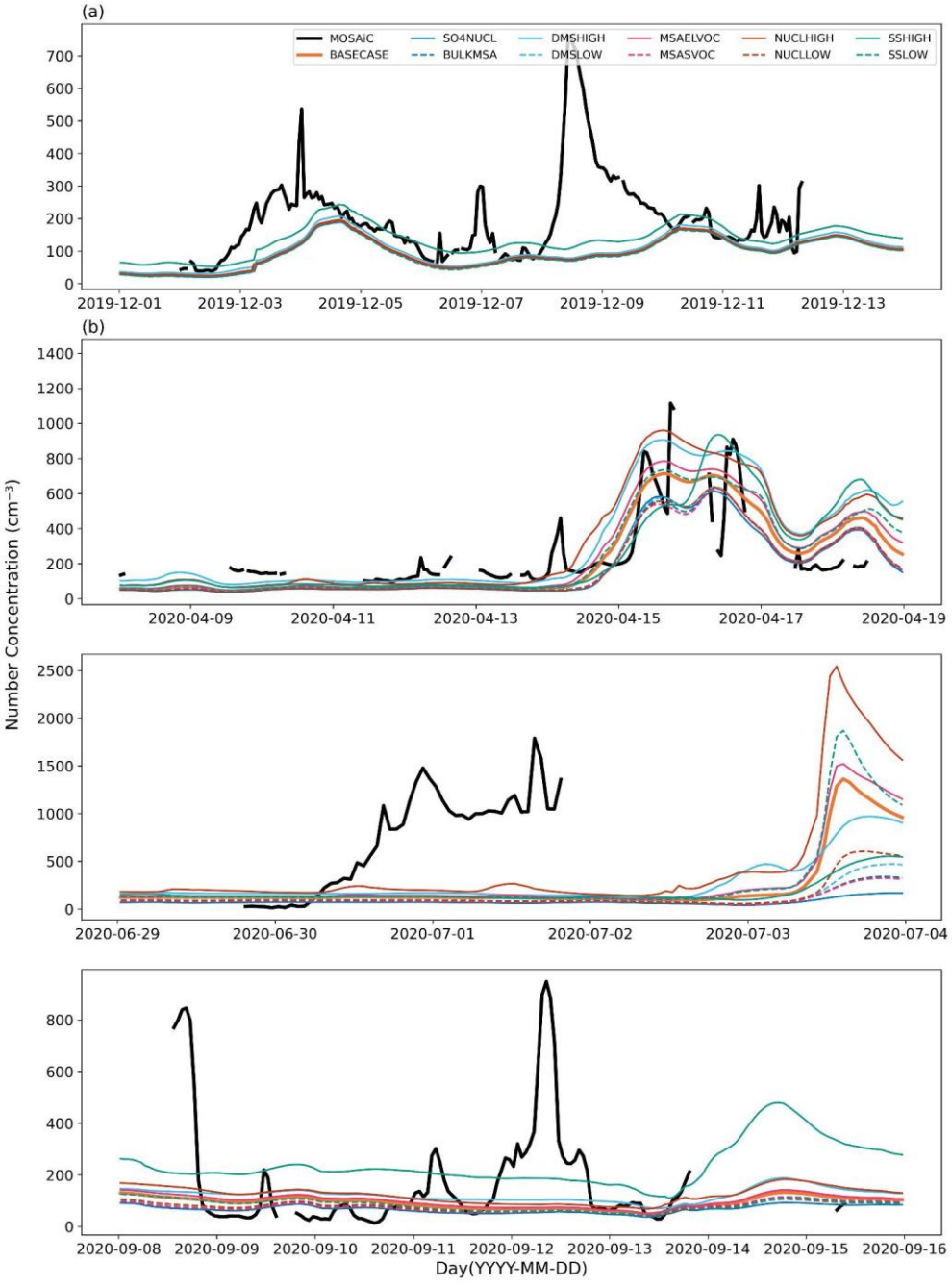

https://doi.org/10.5194/egusphere-2026-2122
Preprint. Discussion started: 27 April 2026

Figure 8: CN values plotted for all 11 simulations and the MOSAiC expedition for 4 aerosol events that occurred during the MOSAiC expedition. The four events are from four different seasons: (a) winter (1 December 2019 – 14 December 2019), (b) spring (8 April 2020 – 19 April 2020), (c) summer (29 June 2020 – 4 July 2020) and (d) autumn (8 September 2020 – 16 September 2020).

Figure 8 shows hourly values of CN concentrations from the MOSAiC expedition measurements and the 11 model simulations. The figure shows a nucleation event that took place between 1 December 2019 and 14 December 2019 (a), 8th April 2020 and 19th April 2020 (b), 29th July 2020 and 4th July 2020(c), and 8th September 2020 and 16th September 2020(d).

Aerosols have a short lifetime in the atmosphere, which makes it important to accurately simulate CN at shorter time scales. Fig. 8a is a blowing snow event that takes place along the MOSAiC track, which has been discussed in detail in Gong et al. (2023). There are two blowing snow events in the time period, one from 2 December 2019 to 6 December 2019 and another shorter one from 7 December 2019 to 8 December 2019. The model seems to behave differently for the two events. We can see that the model captures the first event to some extent, especially in the SS_HIGH. The first period has higher wind speed, which could be the reason for better agreement between the model and observations. However, for the second event, the wind speed is much lower, but a bigger spike in CN is observed. This could be the reason why the model is unable to capture this event. Simple parameterisations which do not include factors other than wind speed and SIC will also not be able to capture this event.

Figure 8b shows CN during a warm air mass intrusion that took place in the Arctic in April 2020; it has been discussed in detail in Dada et al. (2022). Here, a warm air mass is transported from the lower latitudes to the Arctic, bringing aerosols from the lower latitudes. We can see that the model is able to capture this very well. We see a difference between the simulations from 15 April 2020 to 17 April 2020. There are lots of small peaks in the observational data, but in the model, they are seen as two small peaks. In the model, the first peak occurs due to a nucleation event taking place along with the transported aerosols. The simulations, which have a higher nucleation rate than BASECASE – DMS_HIGH, NUCLRATE_HIGH and MSA_ELVOClike, have higher CN. The second peak is due to a strong wind, while all simulations have an increase in CN, the highest impact is on SS_HIGH. While no aerosol event was observed on 18 April 2020, the model simulates a small peak.

Figures 8c and 8d show nucleation events in summer and early autumn. The simulations seem to be unable to capture both of these events. In fig. 8c, from the measurement values, we see an aerosol event taking place. The model does not capture this. However, after a few days, starting from 3 July 2020, we can see that the model produces a nucleation event taking place. This could be the model having the event later than it occurred; we also see a spike in MSA concentration during the same

https://doi.org/10.5194/egusphere-2026-2122
Preprint. Discussion started: 27 April 2026

period (Fig. S4). This could have been a nucleation event that took place as a result. The missing data during that period could also mean there is a different nucleation event taking place. In Fig. 8d, there are multiple small aerosol events taking place. The model does not capture these events. The two events that take place between 9 and 13 September 2020 coincide with an increase in Iodic Acid concentration (Fig. S4). Iodic Acid is a main driver of NPF in late summer and early autumn in the Arctic (Price et al. 2023) and could be the reason the model does not capture these events.

4. Conclusions

In this study, we evaluated the representation of aerosols over the Arctic in global climate models using field observations over the high Arctic. We primarily compared the total aerosol number concentration data between the models and observations to understand the sources of the difference. During the initial comparison with the CMIP6 models, we found very low CN values in the models when compared to observations, whereas TM5 had values closer to observations, especially in summer. Most climate models have aerosol NPF driven by the concentration of sulphuric acid and organic matter. However, in the Arctic, MSA and iodic acid were the dominant aerosol precursor vapours from spring through autumn during the MOSAiC campaign (Boyer et al. 2024). Implementing an MSA-dependent nucleation scheme in TM5 improves the seasonality of the CN values and shows a better correlation with the observations. We also conducted a sensitivity analysis of the model by varying Arctic-relevant aerosol parameters to understand how they affect the CN values. Our results point to missing NPF mechanisms in climate models from late spring to early autumn that affect the total aerosol concentration in the Arctic. When implementing an MSA-dependent nucleation scheme, we observed a significant increase in CN from late spring to summer. These results are in agreement with those of Boyer et al. (2024). We see that nucleation schemes that are only dependent on sulphuric acid or ELVOC are not able to model the CN values during the Arctic expedition and have values close to the CMIP6 models. The current assumption we made about the behaviour of MSA is not ideal. This often results in an overestimation of the CN in the summer. An alternative treatment of MSA volatility is described by Hodshire et al. (2019), where the volatility of MSA is dependent on relative humidity and temperature, and it is treated as ELVOClike, SVOClike, or neither, depending on the conditions. Although the current parameterisation significantly improved the model representation of CN, the CCN concentration was still severely underestimated in the model compared to the observations. The discrepancy between the simulated CN and CCN was highest over the open ocean. This is in agreement with the study by Price et al. (2023), which found similar results when introducing nucleation driven by iodic acid.

Climate models generally overestimate SSA concentrations (Lapere et al. 2023), and we can speculate marine organic matter plays a role in the missing sources of aerosols. Significantly increasing the sea spray emissions in the model produces a CN closer to the observations in summer, but overestimates the values in the autumn months. For this experiment, the values reached their maximum in July and remained high for the next two months. This could be due to these being the

https://doi.org/10.5194/egusphere-2026-2122
Preprint. Discussion started: 27 April 2026

periods with the lowest sea ice cover, resulting in high values of SSA during July-September, as most vapours condense on these particles. As we have seen from Lapere et al. (2023), sea spray emissions are, in general, overestimated in climate models. In our experiments, we see that the CN is sensitive to SSA concentration and its effect on the condensation/coagulation sink. Another result we obtained from our study is the missing source of aerosols in the winter. We see that only the SS_HIGH case, in which we increase the sea spray emissions by a factor of 10, is responsive. All other simulations have values very close to the BASECASE. Some of these are emissions from leads and blowing snow, which have been studied in detail (Lapere et al. 2024; Ranjithkumar et al. 2025).

Aerosols in the Arctic are a complex system with many moving parts, of which only some have been considered in this study because of the model and time constraints. With the variety of data available from the MOSAiC expedition, there are more avenues to be explored to understand the results. A comparison of the size distribution between the model and observations, as well as a detailed comparison with aerosol precursors, is also important. The MOSAiC dataset offers excellent opportunities for evaluating model performance, including size-resolved aerosol distributions and precursor-species comparisons. Future work should jointly examine iodine–MSA nucleation pathways, implement more flexible MSA volatility schemes, assess the role of marine organic aerosol, explore higher-resolution modelling to better capture transient events, and address observational gaps that complicate model evaluation along the drifting MOSAiC track.

Code availability. Code used to generate the plots is available at https://github.com/arundathi-c/mosaic-tm5.git.

Data availability. Data from the MOSAiC campaign is available on PANGAEA at https://doi.org/10.1594/PANGAEA.941886 and https://doi.org/10.1594/PANGAEA.961131.

Author contributions. AC ran the model simulations assisted by TB, KN and MB, and analysed output with guidance from RM and JM. AC, RM and JM contributed to the design of the study. AC prepared the primary text with significant contributions from RM. All authors were involved in finalising the paper. RM was responsible for the acquisition of funding for this project.

Competing interests. There are no competing interests.

Acknowledgements. We acknowledge CSC – IT Centre for Science, Finland, for providing high-performance computing resources. Data used for model evaluation in this manuscript was produced as part of the international Multidisciplinary drifting

https://doi.org/10.5194/egusphere-2026-2122
Preprint. Discussion started: 27 April 2026

Observatory for the Study of the Arctic Climate (MOSAiC) with the tag MOSAiC20192020. We acknowledge the TM5 model consortium for providing the TM5 model framework used in this study.

Financial support. This research has received funding from the European Union's Horizon 2020 research and innovation programme under the grant number 101003826 (CRiceS: Climate Relevant interactions and feedbacks: the key role of sea ice and Snow in the polar and global climate system). TB acknowledges funding from the European Union's Horizon Europe Programme under Grant Agreement No. 101056783 (FOCI). RM acknowledges funding from the European Union's Horizon Europe Programme under Grant Agreement No. 101137639 (CleanCloud).

References

Acosta Navarro, J. C., V. Varma, I. Riipinen, et al. 2016. "Amplification of Arctic Warming by Past Air Pollution Reductions in Europe." *Nature Geoscience* 9 (4): 277–81. https://doi.org/10.1038/ngeo2673.

Adachi, Yukimasa, Seiji Yukimoto, Makoto Deushi, et al. 2013. "Basic Performance of a New Earth System Model of the Meteorological Research Institute (MRI-ESM1)." *Papers in Meteorology and Geophysics* 64: 1–19. https://doi.org/10.2467/mripapers.64.1.

Baccarini, Andrea, Linn Karlsson, Josef Dommen, et al. 2020. "Frequent New Particle Formation over the High Arctic Pack Ice by Enhanced Iodine Emissions." *Nature Communications* 11 (1): 4924. https://doi.org/10.1038/s41467-020-18551-0.

Beck, Lisa J., Nina Sarnela, Heikki Junninen, et al. 2021. "Differing Mechanisms of New Particle Formation at Two Arctic Sites." *Geophysical Research Letters* 48 (4): e2020GL091334. https://doi.org/10.1029/2020GL091334.

Bergman, Tommi, Risto Makkonen, Roland Schrödner, Erik Swietlicki, Vaughan T. J. Phillips, Philippe Le Sager, and Twan Van Noije. 2022. "Description and Evaluation of a Secondary Organic Aerosol and New Particle Formation Scheme within TM5-MP v1.2." *Geoscientific Model Development* 15 (2): 683–713. https://doi.org/10.5194/gmd-15-683-2022.

Bergman, Tommi, Risto Makkonen, Roland Schrödner, Erik Swietlicki, Vaughan T. J. Phillips, Philippe Le Sager, and Twan van Noije. 2022. "Description and Evaluation of a Secondary Organic Aerosol and New Particle Formation Scheme within TM5-MP v1.2." *Geoscientific Model Development* 15 (2): 683–713. https://doi.org/10.5194/gmd-15-683-2022.

Boyer, Matthew, Diego Aliaga, Jakob Boyd Pernov, et al. 2023. "A Full Year of Aerosol Size Distribution Data from the Central Arctic under an Extreme Positive Arctic Oscillation: Insights from the Multidisciplinary Drifting Observatory for the Study of Arctic Climate (MOSAiC) Expedition." *Atmospheric Chemistry and Physics* 23 (1): 389–415. https://doi.org/10.5194/acp-23-389-2023.

Boyer, Matthew, Diego Aliaga, Lauriane L. J. Quéléver, et al. 2024. "The Annual Cycle and Sources of Relevant Aerosol Precursor Vapors in the Central Arctic during the MOSAiC Expedition." *Atmospheric Chemistry and Physics* 24 (22): 12595–621. https://doi.org/10.5194/acp-24-12595-2024.

https://doi.org/10.5194/egusphere-2026-2122
Preprint. Discussion started: 27 April 2026

Cinquini, Luca, Daniel Crichton, Chris Mattmann, et al. 2014. "The Earth System Grid Federation: An Open Infrastructure for Access to Distributed Geospatial Data." *Future Generation Computer Systems*, Special Section: Intelligent Big Data Processing, vol. 36 (July): 400–417. https://doi.org/10.1016/j.future.2013.07.002.

Dada, Lubna, Hélène Angot, Ivo Beck, et al. 2022. "A Central Arctic Extreme Aerosol Event Triggered by a Warm Air-Mass Intrusion." *Nature Communications* 13 (1): 5290. https://doi.org/10.1038/s41467-022-32872-2.

Danabasoglu, G., J. F. Lamarque, J. Bacmeister, et al. 2020. "The Community Earth System Model Version 2 (CESM2)." *Journal of Advances in Modeling Earth Systems* 12 (2): e2019MS001916. https://doi.org/10.1029/2019MS001916.

Emme, Erin J., and Hannah M. Horowitz. 2025. "Impacts of Sea Ice Leads on Sea Salt Aerosols and Atmospheric Chemistry in the Arctic." *Atmospheric Chemistry and Physics* 25 (8): 4531–45. https://doi.org/10.5194/acp-25-4531-2025.

Eyring, Veronika, Sandrine Bony, Gerald A. Meehl, et al. 2016. "Overview of the Coupled Model Intercomparison Project Phase 6 (CMIP6) Experimental Design and Organization." *Geoscientific Model Development* 9 (5): 1937–58. https://doi.org/10.5194/gmd-9-1937-2016.

Gidden, Matthew J., Keywan Riahi, Steven J. Smith, et al. 2019. "Global Emissions Pathways under Different Socioeconomic Scenarios for Use in CMIP6: A Dataset of Harmonized Emissions Trajectories through the End of the Century." *Geoscientific Model Development* 12 (4): 1443–75. https://doi.org/10.5194/gmd-12-1443-2019.

Gong, Xianda, Jiaoshi Zhang, Betty Croft, et al. 2023. "Arctic Warming by Abundant Fine Sea Salt Aerosols from Blowing Snow." *Nature Geoscience* 16 (9): 768–74. https://doi.org/10.1038/s41561-023-01254-8.

Guenther, A. B., X. Jiang, C. L. Heald, et al. 2012. "The Model of Emissions of Gases and Aerosols from Nature Version 2.1 (MEGAN2.1): An Extended and Updated Framework for Modeling Biogenic Emissions." *Geoscientific Model Development* 5 (6): 1471–92. https://doi.org/10.5194/gmd-5-1471-2012.

Hajima, Tomohiro, Michio Watanabe, Akitomo Yamamoto, et al. 2020. "Development of the MIROC-ES2L Earth System Model and the Evaluation of Biogeochemical Processes and Feedbacks." *Geoscientific Model Development* 13 (5): 2197–244. https://doi.org/10.5194/gmd-13-2197-2020.

Heutte, Benjamin, Nora Bergner, Hélène Angot, et al. 2025. "Observations of High-Time-Resolution and Size-Resolved Aerosol Chemical Composition and Microphysics in the Central Arctic: Implications for Climate-Relevant Particle Properties." *Atmospheric Chemistry and Physics* 25 (4): 2207–41. https://doi.org/10.5194/acp-25-2207-2025.

Heutte, Benjamin, Nora Bergner, Ivo Beck, et al. 2023. "Measurements of Aerosol Microphysical and Chemical Properties in the Central Arctic Atmosphere during MOSAiC." *Scientific Data* 10 (1): 690. https://doi.org/10.1038/s41597-023-02586-1.

Hirdman, D., J. F. Burkhart, H. Sodemann, et al. 2010. "Long-Term Trends of Black Carbon and Sulphate Aerosol in the Arctic: Changes in Atmospheric Transport and Source Region Emissions." *Atmospheric Chemistry and Physics* 10 (19): 9351–68. https://doi.org/10.5194/acp-10-9351-2010.

Hodshire, Anna L., Pedro Campuzano-Jost, John K. Kodros, et al. 2019. "The Potential Role of Methanesulfonic Acid (MSA) in Aerosol Formation and Growth and the Associated Radiative Forcings." *Atmospheric Chemistry and Physics* 19 (5): 3137–60. https://doi.org/10.5194/acp-19-3137-2019.

https://doi.org/10.5194/egusphere-2026-2122
Preprint. Discussion started: 27 April 2026

Huijnen, V., J. Williams, M. Van Weele, et al. 2010. "The Global Chemistry Transport Model TM5: Description and Evaluation of the Tropospheric Chemistry Version 3.0." *Geoscientific Model Development* 3 (2): 445–73. https://doi.org/10.5194/gmd-3-445-2010.

Kojoj, Julia, Gabriel Pereira Freitas, Morven Muilwijk, et al. 2024. "An Arctic Marine Source of Fluorescent Primary Biological Aerosol Particles During the Transition from Summer to Autumn at the North Pole." *Tellus B: Chemical and Physical Meteorology* 76 (1). https://doi.org/10.16993/tellusb.1880.

Krol, M., S. Houweling, B. Bregman, et al. 2005. "The Two-Way Nested Global Chemistry-Transport Zoom Model TM5: Algorithm and Applications." *Atmospheric Chemistry and Physics* 5 (2): 417–32. https://doi.org/10.5194/acp-5-417-2005.

Lamarque, J. F., F. Dentener, J. McConnell, et al. 2013. "Multi-Model Mean Nitrogen and Sulfur Deposition from the Atmospheric Chemistry and Climate Model Intercomparison Project (ACCMIP): Evaluation of Historical and Projected Future Changes." *Atmospheric Chemistry and Physics* 13 (16): 7997–8018. https://doi.org/10.5194/acp-13-7997-2013.

Lana, A., T. G. Bell, R. Simó, et al. 2011. "An Updated Climatology of Surface Dimethlysulfide Concentrations and Emission Fluxes in the Global Ocean: UPDATED DMS CLIMATOLOGY." *Global Biogeochemical Cycles* 25 (1): n/a-n/a. https://doi.org/10.1029/2010GB003850.

Lapere, Rémy, Louis Marelle, Pierre Rampal, et al. 2024. "Modeling the Contribution of Leads to Sea Spray Aerosol in the High Arctic." *Atmospheric Chemistry and Physics* 24 (21): 12107–32. https://doi.org/10.5194/acp-24-12107-2024.

Lapere, Rémy, Jennie L. Thomas, Louis Marelle, et al. 2023. "The Representation of Sea Salt Aerosols and Their Role in Polar Climate Within CMIP6." *Journal of Geophysical Research: Atmospheres* 128 (6): e2022JD038235. https://doi.org/10.1029/2022JD038235.

Liu, X., P. L. Ma, H. Wang, et al. 2016. "Description and Evaluation of a New Four-Mode Version of the Modal Aerosol Module (MAM4) within Version 5.3 of the Community Atmosphere Model." *Geoscientific Model Development* 9 (2): 505–22. https://doi.org/10.5194/gmd-9-505-2016.

Malik, Ishfaq Hussain, Rayees Ahmed, James D. Ford, and Abdur Rahim Hamidi. 2025. "Arctic Warming: Cascading Climate Impacts and Global Consequences." *Climate* 13 (5). https://doi.org/10.3390/cli13050085.

Moschos, Vaios, Katja Dzepina, Deepika Bhattu, et al. 2022. "Equal Abundance of Summertime Natural and Wintertime Anthropogenic Arctic Organic Aerosols." *Nature Geoscience* 15 (3): 196–202. https://doi.org/10.1038/s41561-021-00891-1.

Mulcahy, Jane P., Colin Johnson, Colin G. Jones, et al. 2020. "Description and Evaluation of Aerosol in UKESM1 and HadGEM3-GC3.1 CMIP6 Historical Simulations." *Geoscientific Model Development* 13 (12): 6383–423. https://doi.org/10.5194/gmd-13-6383-2020.

Mulcahy, Jane P., Colin G. Jones, Steven T. Rumbold, et al. 2023. "UKESM1.1: Development and Evaluation of an Updated Configuration of the UK Earth System Model." *Geoscientific Model Development* 16 (6): 1569–600. https://doi.org/10.5194/gmd-16-1569-2023.

Noije, T. P. C. van, P. Le Sager, A. J. Segers, et al. 2014. "Simulation of Tropospheric Chemistry and Aerosols with the

https://doi.org/10.5194/egusphere-2026-2122
Preprint. Discussion started: 27 April 2026

Climate Model EC-Earth." *Geoscientific Model Development* 7 (5): 2435–75. https://doi.org/10.5194/gmd-7-2435-2014.

Noije, Twan van, Tommi Bergman, Philippe Le Sager, et al. 2021. "EC-Earth3-AerChem: A Global Climate Model with Interactive Aerosols and Atmospheric Chemistry Participating in CMIP6." *Geoscientific Model Development* 14 (9): 5637–68. https://doi.org/10.5194/gmd-14-5637-2021.

Paasonen, P., T. Nieminen, E. Asmi, et al. 2010. "On the Roles of Sulphuric Acid and Low-Volatility Organic Vapours in the Initial Steps of Atmospheric New Particle Formation." *Atmospheric Chemistry and Physics* 10 (22): 11223–42. https://doi.org/10.5194/acp-10-11223-2010.

Pernov, Jakob Boyd, Eliza Harris, Michele Volpi, et al. 2024. "Pan-Arctic Methanesulfonic Acid Aerosol: Source Regions, Atmospheric Drivers, and Future Projections." *Npj Climate and Atmospheric Science* 7 (1): 166. https://doi.org/10.1038/s41612-024-00712-3.

Petters, M. D., and S. M. Kreidenweis. 2007. "A Single Parameter Representation of Hygroscopic Growth and Cloud Condensation Nucleus Activity." *Atmos. Chem. Phys.*

Previdi, Michael, Karen L. Smith, and Lorenzo M. Polvani. 2021. "Arctic Amplification of Climate Change: A Review of Underlying Mechanisms." *Environmental Research Letters* 16 (9): 093003. https://doi.org/10.1088/1748-9326/ac1c29.

Price, Ruth, Andrea Baccarini, Julia Schmale, et al. 2023. "Late Summer Transition from a Free-Tropospheric to Boundary Layer Source of Aitken Mode Aerosol in the High Arctic." *Atmospheric Chemistry and Physics* 23 (5): 2927–61. https://doi.org/10.5194/acp-23-2927-2023.

Ranjithkumar, Ananth, Eliza Duncan, Xin Yang, et al. 2025. "Direct Observation of Arctic Sea Salt Aerosol Production from Blowing Snow and Modeling over a Changing Sea Ice Environment." *Elementa: Science of the Anthropocene* 13 (1): 00006. https://doi.org/10.1525/elementa.2024.00006.

Rantanen, Mika, Alexey Yu Karpechko, Antti Lipponen, et al. 2022. "The Arctic Has Warmed Nearly Four Times Faster than the Globe since 1979." *Communications Earth & Environment* 3 (1): 168. https://doi.org/10.1038/s43247-022-00498-3.

Riccobono, Francesco, Siegfried Schobesberger, Catherine E. Scott, et al. 2014. "Oxidation Products of Biogenic Emissions Contribute to Nucleation of Atmospheric Particles." *Science* 344 (6185): 717–21. https://doi.org/10.1126/science.1243527.

Saiz-Lopez, Alfonso, Anoop S. Mahajan, Jonathan Abbatt, et al. 2025. "The Influence of Short-Lived Halogens on Atmospheric Chemistry and Climate." *Nature* 648 (8093): 289–99. https://doi.org/10.1038/s41586-025-09753-x.

Schmale, Julia, Paul Zieger, and Annica M. L. Ekman. 2021. "Aerosols in Current and Future Arctic Climate." *Nature Climate Change* 11 (2): 95–105. https://doi.org/10.1038/s41558-020-00969-5.

Shen, Jiali, Wiebke Scholz, Xu-Cheng He, et al. 2022. "High Gas-Phase Methanesulfonic Acid Production in the OH-Initiated Oxidation of Dimethyl Sulfide at Low Temperatures." *Environmental Science & Technology* 56 (19): 13931–44. https://doi.org/10.1021/acs.est.2c05154.

https://doi.org/10.5194/egusphere-2026-2122
Preprint. Discussion started: 27 April 2026

Shupe, Matthew D., Markus Rex, Byron Blomquist, et al. 2022. "Overview of the MOSAiC Expedition: Atmosphere." *Elementa: Science of the Anthropocene* 10 (1): 00060. https://doi.org/10.1525/elementa.2021.00060.

Sihto, S. L., M. Kulmala, V. M. Kerminen, et al. 2006. "Atmospheric Sulphuric Acid and Aerosol Formation: Implications from Atmospheric Measurements for Nucleation and Early Growth Mechanisms." *Atmospheric Chemistry and Physics* 6 (12): 4079–91. https://doi.org/10.5194/acp-6-4079-2006.

Sipilä, Mikko, Torsten Berndt, Tuukka Petäjä, et al. 2010. "The Role of Sulfuric Acid in Atmospheric Nucleation." *Science* 327 (5970): 1243–46. https://doi.org/10.1126/science.1180315.

Spiro, Peter A., Daniel J. Jacob, and Jennifer A. Logan. 1992. "Global Inventory of Sulfur Emissions with 1°×1° Resolution." *Journal of Geophysical Research: Atmospheres* 97 (D5): 6023–36. https://doi.org/10.1029/91JD03139.

Stier, P., J. Feichter, S. Kinne, et al. 2005. "The Aerosol-Climate Model ECHAM5-HAM." *Atmos. Chem. Phys.*

Takemura, Toshihiko, Toru Nozawa, Seita Emori, Takashi Y. Nakajima, and Teruyuki Nakajima. 2005. "Simulation of Climate Response to Aerosol Direct and Indirect Effects with Aerosol Transport-Radiation Model." *Journal of Geophysical Research: Atmospheres* 110 (D2). https://doi.org/10.1029/2004JD005029.

Tanaka, Taichu Y., Kohtaro Orito, Tsuyoshi T. Sekiyama, Kiyotaka Shibata, Masaru Chiba, and Hiroshi Tanaka. 2003. "MASINGAR, a Global Tropospheric Aerosol Chemical Transport Model Coupled with MRI/JMA98 GCM." *Papers in Meteorology and Geophysics* 53 (4): 119–38. https://doi.org/10.2467/mripapers.53.119.

Tang, Jing, Putian Zhou, Paul A. Miller, et al. 2023. "High-Latitude Vegetation Changes Will Determine Future Plant Volatile Impacts on Atmospheric Organic Aerosols." *Npj Climate and Atmospheric Science* 6 (1): 147. https://doi.org/10.1038/s41612-023-00463-7.

Van Noije, T. P. C., P. Le Sager, A. J. Segers, et al. 2014. "Simulation of Tropospheric Chemistry and Aerosols with the Climate Model EC-Earth." *Geoscientific Model Development* 7 (5): 2435–75. https://doi.org/10.5194/gmd-7-2435-2014.

Vignati, Elisabetta, Julian Wilson, and Philip Stier. 2004. "M7: An Efficient Size-Resolved Aerosol Microphysics Module for Large-Scale Aerosol Transport Models: AEROSOL MICROPHYSICS MODULE." *Journal of Geophysical Research: Atmospheres* 109 (D22): n/a-n/a. https://doi.org/10.1029/2003JD004485.

Vuuren, Detlef P. van, Jae Edmonds, Mikiko Kainuma, et al. 2011. "The Representative Concentration Pathways: An Overview." *Climatic Change* 109 (1): 5. https://doi.org/10.1007/s10584-011-0148-z.

Williams, Jason E., K. Folkert Boersma, Phillipe Le Sager, and Willem W. Verstraeten. 2017. "The High-Resolution Version of TM5-MP for Optimized Satellite Retrievals: Description and Validation." *Geoscientific Model Development* 10 (2): 721–50. https://doi.org/10.5194/gmd-10-721-2017.

Yukimoto, Seiji, Hideaki Kawai, Tsuyoshi Koshiro, et al. 2019. "The Meteorological Research Institute Earth System Model Version 2.0, MRI-ESM2.0: Description and Basic Evaluation of the Physical Component." *Journal of the Meteorological Society of Japan. Ser. II* 97 (5): 931–65. https://doi.org/10.2151/jmsj.2019-051.